Plant Physiology®

Plant Physiology, 2025, **198**, kiaf327
https://doi.org/10.1093/plphys/kiaf327
Advance access publication 23 July 2025
Research Article

C_4 plants respond to phosphate starvation differently than C_3 plants

Raissa Krone,[1] Silke Gerlich,[1,†] Mette Mertens,[1] Anna Koprivova,[1] Philipp Westhoff,[2] Stanislav Kopriva[1,*]

[1]Institute for Plant Sciences, Cluster of Excellence on Plant Sciences (CEPLAS), University of Cologne, Zülpicher Str. 47b, Cologne 50674, Germany
[2]Plant Metabolism and Metabolomics Facility, Cluster of Excellence on Plant Sciences (CEPLAS), Heinrich Heine University, Düsseldorf 40225, Germany
*Author for correspondence: skopriva@uni-koeln.de
[†]Present address: Institute for Advanced Simulation, Forschungszentrum Jülich, 52428 Jülich.
The author responsible for distribution of materials integral to the findings presented in this article in accordance with the policy described in the Instructions for Authors (https://academic.oup.com/plphys/pages/General-Instructions) is: Stanislav Kopriva (skopriva@uni-koeln.de).

Abstract

C_4 photosynthesis concentrates CO_2 around Rubisco, thereby decreasing photorespiration and leading to greater productivity. C_4 photosynthesis evolved several times independently in different plant families including monocots and dicots. Besides changes in carbon fixation, C_4 plants have also evolved several alterations in nitrogen and sulfur nutrition, leading to better nitrogen use efficiency. Here, we utilized C_3 and C_4 species from 2 model systems, *Flaveria* and *Panicum*, to ask whether the evolution of C_4 photosynthesis also affected phosphate homeostasis. The accumulation of phosphate within the plant shifted from the roots to the shoots with the evolution of C_4, which can probably be explained by the higher demand of phosphate for completing the C_4 cycle. A limitation of carbon assimilation by phosphate availability was shown solely for the C_4 dicot plant, indicating a higher sensitivity to starvation. Metabolic responses to phosphate limitation, including accumulation of amino acids, TCA cycle intermediates, and starch, were genus or species specific, rather than associated with the photosynthesis type. The expression of key phosphate starvation response genes was induced in all species by phosphate deficiency, while the high induction of microRNA399 coupled with a repression of *PHOSPHATE 2 (PHO2)* was especially prominent in the C_4 monocot. Thus, it seems that C_4 photosynthesis increases the demand for phosphate in the leaves and C_4 plants either respond more strongly to phosphate deficiency than C_3 plants or experience inhibition of photosynthesis.

Introduction

As human population is growing, the global demand for nutritious food is increasing, while at the same time, rising temperatures and elevated frequency of extreme weather events due to climate change lead to high yield losses in the agriculture (van Dijk et al. 2021; Rezaei et al. 2023). However, the C_4 photosynthetic mechanism offers a powerful tool to enhance plant productivity, and thus, engineering the C_4 cycle into C_3 crops such as rice (*Oryza sativa*) would be a promising approach to meet the future demand for food (Ermakova et al. 2020).

C_4 photosynthesis is a mechanism to minimize oxygenation of Rubisco and concentrate CO_2 around the enzyme by splitting the CO_2 assimilation between 2 cell types: mesophyll and bundle sheath cells (Slack et al. 1969; Hatch 1987; Sage 2004). Primary CO_2 fixation takes place in the mesophyll, resulting in the organic acids malate and aspartate, which are transported to the bundle sheath where they are decarboxylated and the released CO_2 is then assimilated by Rubisco in the Calvin cycle (Hatch 1987). This results in minimizing energetically wasteful photorespiration and thus leads to a greater productivity of C_4 plants. The biochemical division of function is accompanied by a so-called Kranz anatomy of the leaves, characterized by an inner bundle sheath and an outer mesophyll layer surrounding the veins (Lundgren et al. 2014).

The C_4 photosynthesis evolved more than 60 times independently in various families of monocots and dicots under favoring conditions including a low atmospheric CO_2, hot temperatures, and a dry environment (Sage 2004). The evolution was a stepwise process, which led to a series of C_3–C_4 intermediate species possessing anatomical and biochemical characteristics that are situated between these of C_3 and C_4 plants (Kennedy and Laetsch 1974). A good model to study the C_4 cycle and its evolution is the genus *Flaveria*, in which C_4 evolved at least twice inside the same genus itself (Powell 1978). Furthermore, among the *Flaveria* genus, there are not only clear C_3 and C_4 species but also a range of stable C_3–C_4 intermediate and C_4-like species (Ku et al. 1991). Besides several evolution events in dicots, C_4 photosynthesis also evolved in 3 monocot families including prominent crop plants such as maize as well as grass species of the *Panicum* genus. *Panicum* species are another convenient model to study C_4 development, as they also include C_3, C_4, and C_3–C_4 intermediate species (Edwards and Gutierrez 1972; Sternberg et al. 1986).

The increasing atmospheric CO_2 concentrations can enhance the photosynthetic CO_2 fixation in many crop plants, namely, those with C_3 photosynthetic mechanisms. However, while yields may increase with higher CO_2, the levels of proteins and mineral nutrients essential for human health are decreasing in crop plants such as rice or wheat (Loladze 2014; Zhu et al. 2018;

Received April 28, 2025. Accepted June 17, 2025.

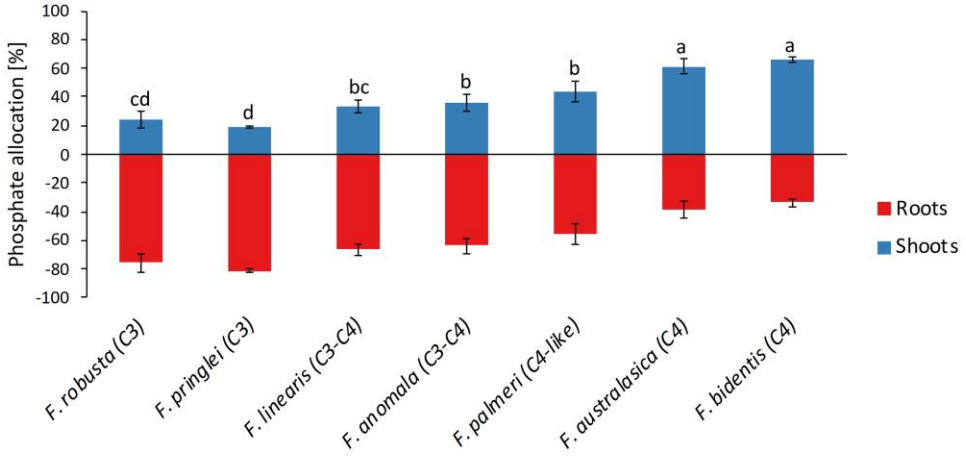

Figure 1. Allocation of inorganic phosphate from the roots to the leaves increases along the evolutionary gradient of *Flaveria* species. Percentage of total phosphate content in roots and shoots of 7 *Flaveria* species was analyzed 23 d after germination by using ion chromatography. Data are shown as mean and standard deviation, while letters represent significant differences ($P < 0.05$) based on a 1-way ANOVA followed by a Tukey's HSD test ($n = 4$).

Jobe et al. 2019). Hence, it is important to understand the integration of carbon metabolism with mineral nutrition in plants. This is particularly important for C_4 plants that are much less studied in terms of mineral nutrition, although the C_4 photosynthetic mechanism leads to several adaptations in nutrient assimilation (Jobe et al. 2019).

Indeed, besides spatial separation of carbon assimilation, C_4 plants also show spatial separation of assimilation of key mineral nutrients nitrogen and sulfur. While nitrate reduction to ammonia takes place exclusively in the mesophyll of C_4 plants (Moore and Black 1979), enzymes for sulfate reduction are localized in the bundle sheath cells (Gerwick et al. 1980), at least in C_4 monocots (Koprivova et al. 2001). Furthermore, C_4 plants have a higher nitrogen use efficiency, presumably due to lower accumulation of Rubisco (Sage et al. 1987), and the demand for reduced sulfur is increasing with increasing establishment of the C_4 cycle in *Flaveria* species (Gerlich et al. 2018). While there is clear evidence of adaptive changes in nitrate and sulfate nutrition in the evolution of C_4 photosynthesis, very little is known in this context about another key nutrient, phosphate.

Plants take up inorganic phosphate, which is essential as a building block of ATP, nucleic acids, and phospholipids and in regulatory mechanisms including phosphorylation (Maathuis 2009). Also, several enzymes involved in the C_4 cycle are regulated via phosphorylation, among them the CO_2 assimilating enzyme phosphoenolpyruvate (PEP) carboxylase as well as pyruvate phosphate dikinase (PPDK), responsible for the recycling of pyruvate back to PEP (Jiao and Chollet 1991; Vidal and Chollet 1997). Furthermore, phosphate is essential for the activity of the triose-phosphate/phosphate translocator (TPT) which interchanges phosphate and triose-phosphates between the cytosol and chloroplasts (Fliege et al. 1978). This transporter is especially important in the C_4 cycle, as it is responsible for exporting PEP from the chloroplast (Heldt et al. 1991).

Hence, this study focuses on the differences in phosphate nutrition between closely related C_3 and C_4 plants in order to address the impact of C_4 cycle on phosphate nutrition and to assess if changes in phosphate nutrition were necessary for a successful evolution of C_4 photosynthesis. We investigated plants from the monocot genus *Panicum* and the dicot *Flaveria*, spanning a big evolutionary distance, with the aim of unraveling similarities and differences between the monocots and dicots in the effect of the photosynthesis type on phosphate homeostasis.

Results

Phosphate allocation between roots and shoots in *Flaveria* species with a different photosynthesis type

We have shown previously a gradient in concentration of sulfur metabolites from C_3 to C_4 *Flaveria* species (Koprivova et al. 2001; Gerlich et al. 2018). We, therefore, asked whether there is a similar gradient in phosphate content among the *Flaveria* species. There was no relation between phosphate content in roots or shoots and the degree of C_4 photosynthesis in 7 *Flaveria* species conducting different types of photosynthesis (Supplementary Fig. S1A). However, when comparing the allocation of phosphate between the roots and shoots of these species, an interesting trend along the evolutionary gradient was observed. The relative phosphate content (calculated from total phosphate content [Supplementary Fig. S1A]) in shoots was increasing from C_3 over C_3–C_4 and C_4-like toward C_4 species, while the relative phosphate content in the root was decreasing (Fig. 1). Hence, there seems to be a shift in phosphate allocation from roots to shoots along the evolutionary gradient, and the translocation of phosphate from the roots to the shoots seems to increase with a higher degree of C_4 mechanism. When total phosphorus was analyzed, a similar result was observed with increasing proportion of P in shoots toward C_4 plants (Supplementary Fig. S1, B and C). These results show that also phosphate nutrition might be affected during evolution of C_4 photosynthesis and suggest a higher demand for phosphate in the leaves of plants performing the C_4 cycle.

To find out how the different allocation of phosphate between shoots and roots is controlled, interspecific grafts between a C_3 species (*Flaveria robusta*) and a C_4 species (*Flaveria bidentis*) were generated (as described in Gerlich et al. 2018) and phosphate content was determined. The distribution of phosphate between the organs was controlled by the identity of the shoot. The C_3/C_4 graft as well as the C_3/C_3 homograft control accumulated higher PO_4 levels in their roots than in the shoots, while the C_4/C_3 and the C_4/C_4 grafts had higher phosphate in the shoots (Fig. 2). However, the overall phosphate concentrations were higher in grafts with C_4 rootstock than in those with C_3 roots. This was also confirmed by measuring the phosphate uptake rates of the grafts (Supplementary Fig. S2), which was higher in individuals that possessed a C_4 shoot, indicating that this was the responsible organ for an increased translocation of phosphate into the leaves. However, while it seems that allocation between the organs is

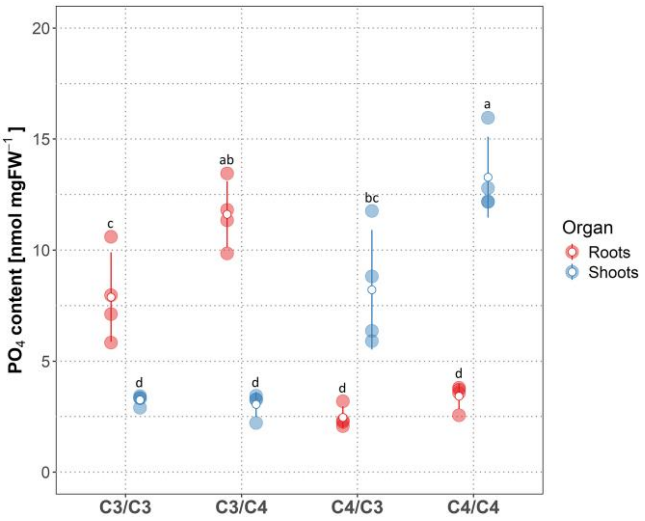

Figure 2. Phosphate content in roots and shoots of interspecific grafts between *F. robusta* (C_3) and *F. bidentis* (C_4). Seedlings were grafted 5 d after germination, while samples were harvested 35 d after grafting. Phosphate content was measured by ion chromatography. Graph shows individual measurements as well as their mean and SD ($n = 4$). Letters indicate significant differences ($P < 0.05$) based on a 2-way ANOVA followed by a Tukey's HSD test.

driven by the shoot, the C_4 roots have a higher capacity to take up and translocate phosphate than the C_3 roots.

Effect of phosphate supply on growth and P homeostasis of C_3 and C_4 plants

To better understand the interconnection of phosphate homeostasis and the type of photosynthesis, we compared the effects of phosphate deficiency on closely related C_3 and C_4 species in more detail. Since sulfate assimilation is organized differently in C_4 dicots and monocots (Koprivova et al. 2001), we included representatives of both, *F. robusta* and *F. bidentis* as well as *Panicum bisulcatum* (C_3) and *Panicum miliaceum* (C_4), respectively. As a first indicator of the plant performance under different phosphate regimes, the biomass production was determined. However, only a slight increase of the fresh weight under intermediate phosphate conditions was observed in all species, while the decrease of fresh weight under low phosphate conditions was most prominent in *F. bidentis* (Supplementary Fig. S3). When comparing the ratio of biomass between roots and shoots, it is notable that the root-to-shoot ratio of *P. bisulcatum* was higher under low phosphate, indicating that these plants invest more into their root growth under phosphate stress or that the low phosphate availability inhibits shoot growth.

Then, we determined the effect of the decreased P supply on phosphate accumulation. The concentrations of phosphate in roots and shoots were generally proportional to the phosphate supply in the media; however, there were some variations in different species especially in the allocation between shoots and roots. In the 2 *Flaveria* species, there were no differences between C_3 and C_4 under low phosphate conditions, but under a sufficient supply, the C_3 species had higher phosphate levels in the roots, while the C_4 species showed a similar accumulation in the shoots and roots (Fig. 3A). Also, in the 2 *Panicum* species, there were no differences between the C_3 and C_4 under phosphate starvation. However, at higher phosphate supply, both *Panicum* species had higher phosphate concentration in the shoot than in the root, this ratio being higher in C_4 species *P. miliaceum* (Fig. 3B). The shoot/root ratios calculated from these results confirm these observations (see Supplementary Fig. S4).

Next, we determined the contents of total phosphorus in plants grown in a gradient of P supply. The measurements of total phosphorus agreed largely with the results obtained for the phosphate contents, with an overall increasing amount of phosphorus under increasing availability of phosphate (Fig. 3, C and D). Under low phosphate conditions, total phosphorus levels were similar between roots and shoots in all 4 species. However, under high phosphate concentrations, the phosphorus pool increased especially in the roots of *Flaveria* and shoots of *Panicum*, showing a clear difference in allocation between the genera. At the same time, the *Flaveria* C_3 and the *Panicum* C_4 showed overall greatly increased phosphorus levels in comparison to their respective relative species.

We then determined phosphate uptake, using radioactively labeled phosphate (^{33}P). Interestingly, the measurement indicated a substantial increase of phosphate uptake rate under a low phosphate supply in both C_3 species, *F. robusta* and *P. bisulcatum*, while it remained unaffected in both C_4 species (Fig. 4). As suggested by the analyses of the grafts (Supplementary Fig. S2), there was a tendency of a higher uptake rate at normal supply in C_4 *F. bidentis*, but this was not significant on the chosen level of $P < 0.05$. In *Panicum*, however, in control conditions, the C_4 species showed a higher uptake rate than the C_3 species (Fig. 4).

Effect of P deficiency on photosynthetic performance

We were then interested to test whether there is any difference between C_3 and C_4 species in the physiological effects of phosphate deficiency. Therefore, as a measure of the photosynthetic performance, CO_2 response curves were recorded for the different species grown under control or low phosphate conditions (Fig. 5). The initial slopes of the curves and the resulting CO_2 compensation points were higher in both C_4 species compared to their C_3 relatives, reflecting the generally higher carboxylation efficiency of C_4 plants. However, no effect of the phosphate deficiency on the curve progressions under low CO_2 concentrations could be detected. From the plateau phase of the assimilation curves, the maximal assimilation rate for each species under low phosphate or control conditions was calculated. This rate was similar between C_3 and C_4 relatives under normal conditions. However, in the C_4 *F. bidentis*, the maximal rate decreased significantly when plants were exposed to low phosphate conditions (Fig. 5C). In the other 3 species, there were no significant differences between the treatments. Thus, it seems that in the dicot genus *Flaveria*, phosphate deficiency affects the C_4 species more strongly than the C_3 species, but in the monocots, the effect is not apparent (Fig. 5D).

Effects of P starvation on metabolic profiles in C_3 and C_4 plants

Given the effect of phosphate starvation on photosynthesis, we determined the concentrations of various metabolites under these conditions. Gas chromatography-mass spectrometry (GC-MS) analyses of shoot materials revealed distinct differences among the 4 species and in their response to P starvation. The heatmap in Fig. 6 shows relative changes in the metabolite levels in response to the low phosphate treatment calculated from the absolute amounts under the 2 conditions (Supplementary Table S1). The response of the accumulation of the majority of metabolites to phosphate starvation, including amino acids,

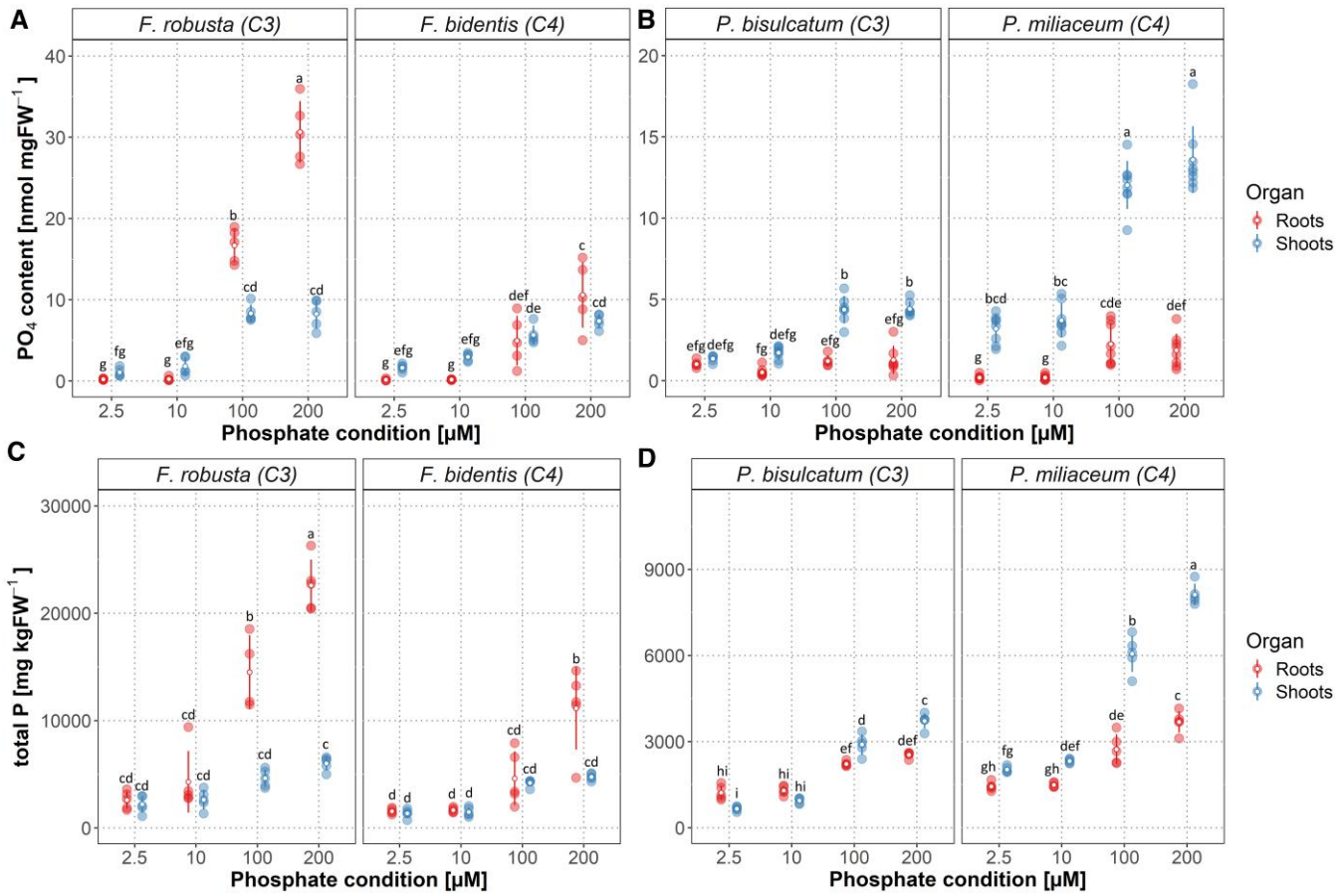

Figure 3. Phosphate and phosphorus contents in the plants reflect phosphate availability in the growth media. Roots and shoots were harvested separately after 4 wk in the respective phosphate treatment for *F. robusta* and *F. bidentis* **A** and **C)** and after 2 wk for *P. bisulcatum* and *P. miliaceum* **B** and **D)**. Phosphate content was determined via ion chromatography, while total phosphorus levels were measured using ICP-MS. Graphs show individual measurements as well as their mean and standard deviation ($n = 5$ to 8). Letters indicate significant differences ($P < 0.05$) based on a 3-way ANOVA followed by a Tukey's HSD test.

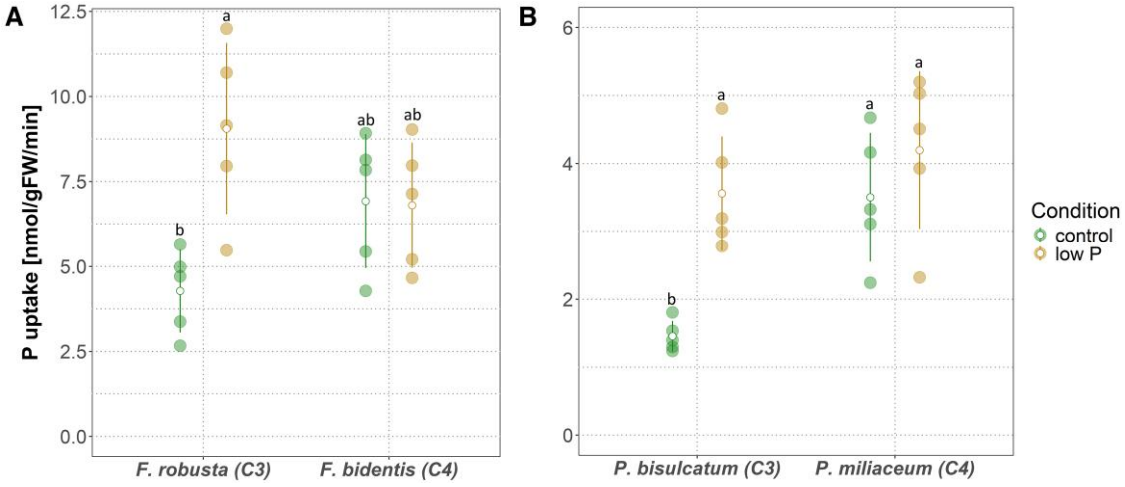

Figure 4. Phosphate uptake rate is induced by low phosphate treatment in C_3 species. Phosphate uptake was measured in *F. robusta* and *F. bidentis* **A)** and *P. bisulcatum* and *P. miliaceum* **B)** grown for 7 d under low P (2.5 µM) or control (200 µM) conditions by feeding them with $^{33}PO_4$ for 20 min. The uptake was quantified via a scintillation counter. Graphs show individual measurements as well as their mean and SD ($n = 5$). Letters indicate significant differences ($P < 0.05$) based on a 2-way ANOVA followed by a Tukey's HSD test.

TCA cycle intermediates, and sugars, showed opposite trends in *Flaveria* and *Panicum*. While these metabolites tended to be less abundant after P starvation in *Flaveria*, they accumulated more in *Panicum*.

The levels of several amino acids, such as glutamate, alpha-alanine, 5-oxoproline, and valine, were decreased by phosphate starvation in both *Flaveria* species, while several others (aspartate, phenylalanine, methionine, glutamine, leucine, and

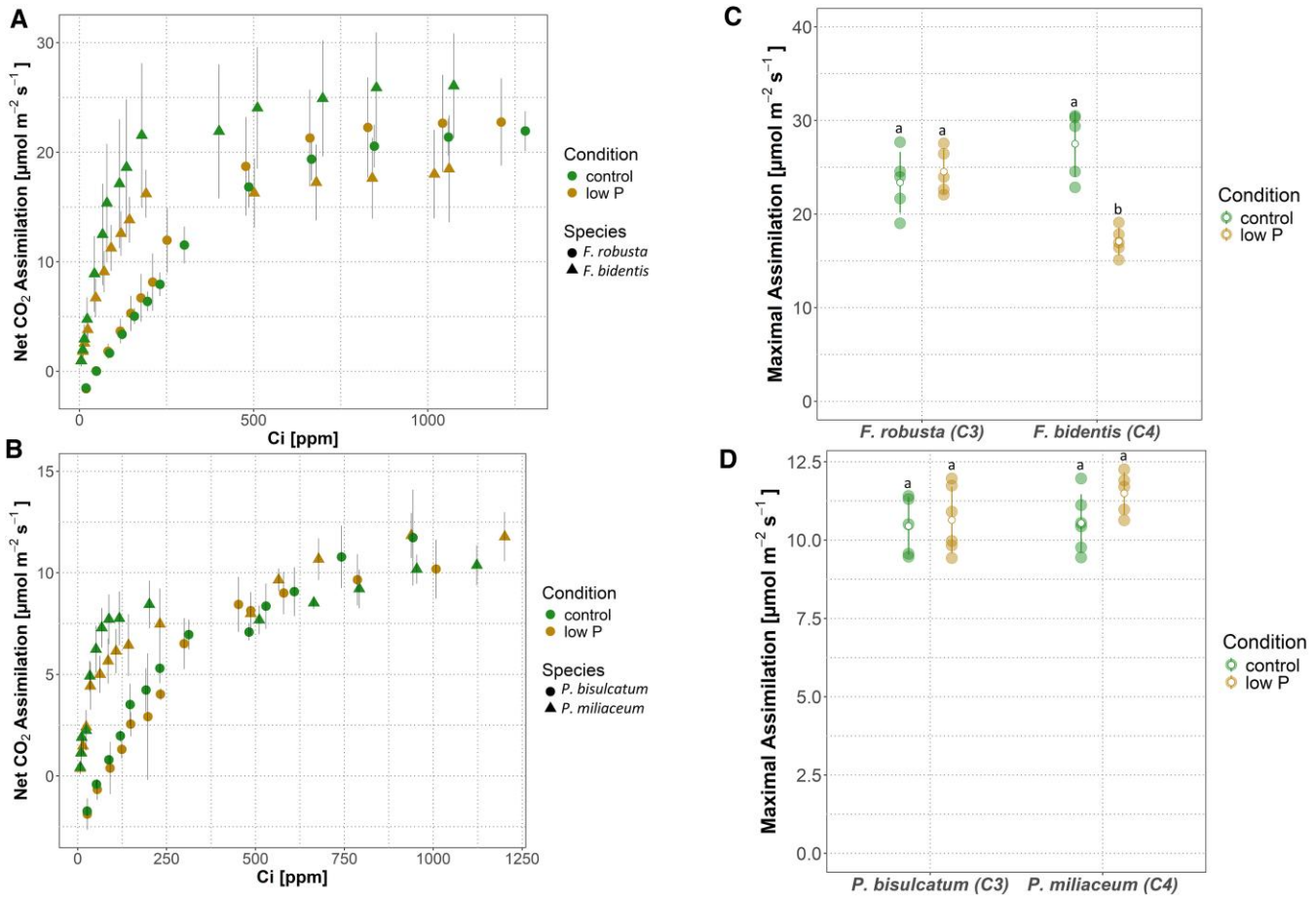

Figure 5. Photosynthetic performance under phosphate starvation. CO_2 assimilation was determined by an infrared gas analyzer supplying the leaf with increasing CO_2 conditions. Plants were grown for 4 wk (*Flaveria*) or 2 wk (*Panicum*) under low phosphate (2.5 µM) or control (200 µM) conditions, before the last fully expanded leaf was used for the measurement. **A** and **B)** The CO_2 assimilation rates over increasing internal CO_2 concentrations presented as means and SD of 5 to 6 biological replicates. The maximal assimilation rate **C** and **D)** was calculated based on these curves as the maximal measured value for each replicate presented as individual data points and including means (empty circle) and standard deviations. Letters indicate statistically significant differences ($P < 0.05$) based on a 2-way ANOVA followed by a Tukey's HSD test.

serine) were significantly less abundant, specifically in *F. robusta*. On the other hand, in both *Panicum* species, most amino acids showed a tendency of increased levels under phosphate starvation; however, that was significant only for phenylalanine in *P. bisulcatum*. With the exception of raffinose, all sugars showed the same general trend of decreased levels under phosphate limitation in both *Flaveria* species and increased levels in both *Panicum* species. Several intermediates of the TCA cycle, including early steps such as pyruvate, steps from in between such as alpha-ketoglutarate, and late steps such as fumarate and malate, accumulated to a significantly lower amount in the C_4 *Flaveria*, while they remained unaffected in its C_3 relative. This suggests that in dicot species, TCA cycle is more affected by the phosphate limitation in C_4 than in C_3 species. In *Panicum*, different steps of the TCA cycle were affected in C_3 and C_4, but TCA intermediates were increased differently in the 2 species. While malate and citrate showed elevated levels in *P. bisulcatum*, pyruvate, alpha-ketoglutarate, and fumarate accumulated to higher levels in *P. miliaceum*. Thus, the effect of P deficiency on the TCA cycle seems to be stronger in the C_4 dicot than in monocot.

Overall, it seems that the changes in the metabolite levels are not specific for the photosynthesis type but rather specific for the monocots and dicots, indicating clearly distinct coping strategies with phosphate limitation on a metabolic level between these genera as they often showed opposite regulation of metabolite levels.

Apart from the different metabolites determined by GC-MS, other compounds and nutrients were determined in P-deficient plants. Firstly, we measured starch, which plants use to store sugars as an output of photosynthesis. Starch levels at the end of the day showed differences between the species already under control conditions in the dicots. The C_4 species *F. bidentis* had a lower starch content compared to its C_3 relative (Fig. 7A). The accumulation of starch was significantly increased under phosphate starvation in comparison to control conditions in *F. bidentis* and *P. bisulcatum*, while there was only a slight increase in *P. miliaceum* and no changes in *F. robusta*.

Additionally, we determined the levels of anions: nitrate and sulfate. Nitrate content in *Flaveria* was decreasing with higher phosphate supply, but this was not the case for *Panicum* (Supplementary Fig. S5). On the other hand, sulfate levels were slightly increasing with a higher phosphate availability in *Panicum*, at least in the roots, while they remained largely unaffected in *Flaveria* (Supplementary Fig. S6). When comparing the overall concentrations between the plants of different photosynthesis types, nitrate was more abundant in shoots of C_3 *Flaveria* than of C_4, while sulfate showed higher levels in the shoots of C_3 *Flaveria* and roots of C_4 *Panicum* in comparison to their counterpart species.

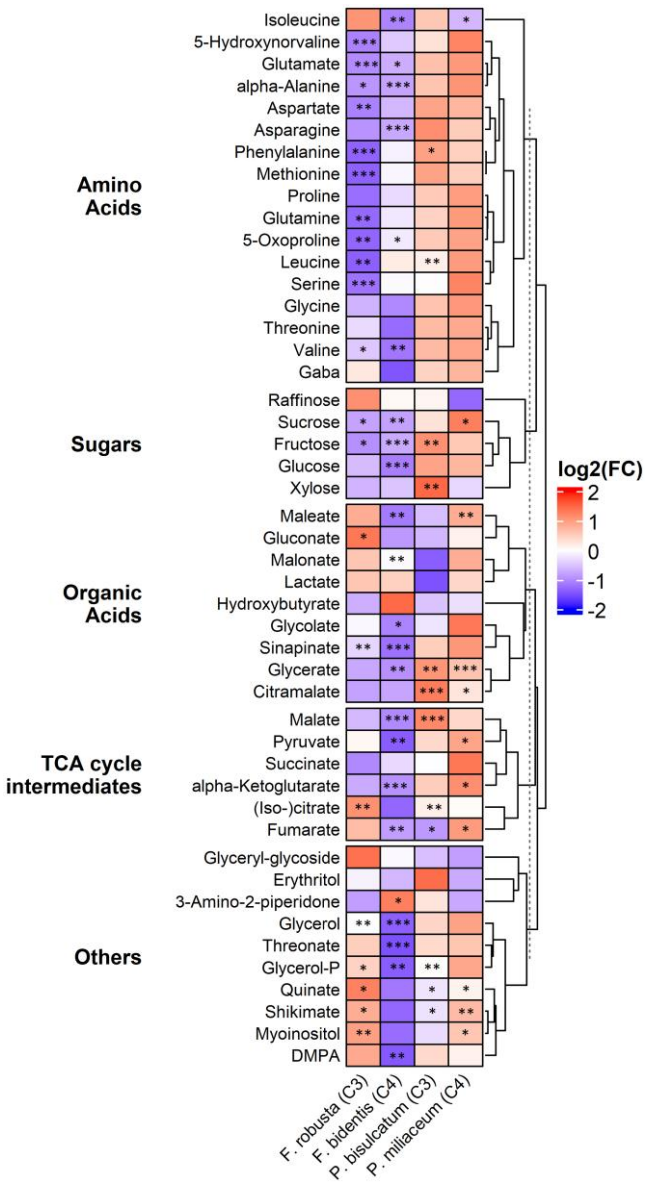

Figure 6. Regulation of individual metabolite levels by phosphate limitation. Plants were grown for 4 wk (*Flaveria*) or 2 wk (*Panicum*) under low phosphate (2.5 μM) or control (200 μM) conditions, before the leaf material was used for metabolic profiling via GC-MS. Heatmap presents the mean relative changes of the content under low phosphate conditions in comparison to the control ($n = 5$). Asterisks indicate significant changes between the treatments based on a Student's *t*-test (*$P < 0.05$; **$P < 0.01$; ***$P < 0.001$).

Accumulation of further mineral nutrients was determined via inductively coupled plasma mass spectrometry (ICP-MS) to assess the effects of P deficiency on the ionome (summarized in heatmaps in Supplementary Fig. S7). However, there were no dramatic changes in element contents, and the levels were relatively stable especially in the shoots. Iron accumulation, which is known to be dependent on the presence of phosphate (Yang et al. 2024), was significantly lower under phosphate starvation in *F. bidentis* (Supplementary Fig. S8). Manganese, which is involved in the water splitting of photosystem 2 (Oliver et al. 2022), was clearly less abundant in the phosphate-starved roots of *F. bidentis*, while there was a slight decrease in both *Panicum* species (Supplementary Fig. S9).

Transcriptional response to phosphate deficiency

To evaluate the different responses to phosphate limitation on a transcriptional level, the expression of key genes involved in the phosphate starvation response was quantified. *PHOSPHATE 1* (*PHO1*), encoding a phosphate transporter that is responsible for the phosphate loading into the xylem, was much more highly expressed in both C_4 species compared to their C_3 relatives (Fig. 8A). However, *PHO1* was not transcriptionally regulated under phosphate starvation. PHO1 is under posttranscriptional negative control by an E2 ubiquitin conjugase encoded by the *PHOSPHATE 2* (*PHO2*) gene. The *PHO2* transcript levels were much lower in C_4 *Flaveria* than in C_3, but this big difference was not conserved in *Panicum* (Fig. 8B). Under low phosphate conditions, *PHO2* was downregulated only in *P. miliaceum* (Fig. 8B). As expected, genes for one of the main phosphate transporter family PHT1 were transcriptionally induced by phosphate starvation in all 4 tested species (Fig. 8C), indicating that this part of the phosphate starvation is strictly conserved. The same was true for genes involved in the synthesis of sulfolipid. It was shown earlier that phosphate limitation increases sulfolipids while decreasing phospholipids and the enzymes in sulfolipid synthesis UDP-sulfoquinovose synthase (SQD1) and sulfoquinovosyl transferase (SQD2) are the key factors in such lipid reprogramming (Essigmann et al. 1998). Here, we used *SQD1* for *Panicum* and *SQD2* for *Flaveria* since their sequences were respectively better conserved among species. The gene expression was induced by low phosphate in all 4 species (Fig. 8D).

To get a more mechanistic understanding of the induction of the phosphate starvation response in the different species, expression of microRNA399, a key regulator in the phosphate homeostasis, was quantified. A slight induction by the low phosphate treatment was observed in all of the species; however, in *P. miliaceum*, the expression was induced on average around 500 times, which was drastically more than in any of the other species (Fig. 8E).

Discussion

PO4 accumulation shifts from the roots to the shoots during C_4 evolution

A sufficient supply with macro- and micronutrient is essential for plant growth and can have a huge impact on crop yield (Maathuis 2009; Mueller et al. 2012). This makes it a crucial research field to understand how to attain our future agricultural needs, especially in the context of C_4 plants, which generally have a higher productivity (Atkinson et al. 2016). Nitrate and sulfate assimilation were shown to be spatially separated in C_4 plants. While nitrate is assimilated in the mesophyll cells, the first steps of sulfate assimilation take place in bundle sheath cells of C_4 monocots (Jobe et al. 2020). Regarding nitrate, C_4 plants are able to cope better with deficiency since their nitrate use efficiency is higher than in C_3 plants (Sage et al. 1987). Previous studies focusing on the sulfur homeostasis during C_4 evolution in *Flaveria* revealed a higher demand for sulfate reduction with a higher degree of C_4 within the genus, while the uptake and distribution of sulfate were shown to be under the control of the identity of the shoot (Koprivova et al. 2001; Gerlich et al. 2018). However, knowledge about phosphate assimilation and deficiency response in C_4 plants is still limited. Hence, this study focuses on the phosphate homeostasis during C_4 evolution in monocots and dicots, and we could indeed detect some substantial differences between closely related C_3 and C_4 plants.

In *Flaveria*, phosphate allocation shifted from a high proportion in the roots toward the shoots along the gradient from C_3 to C_4 species (Fig. 1). These observations in the dicot *Flaveria* were

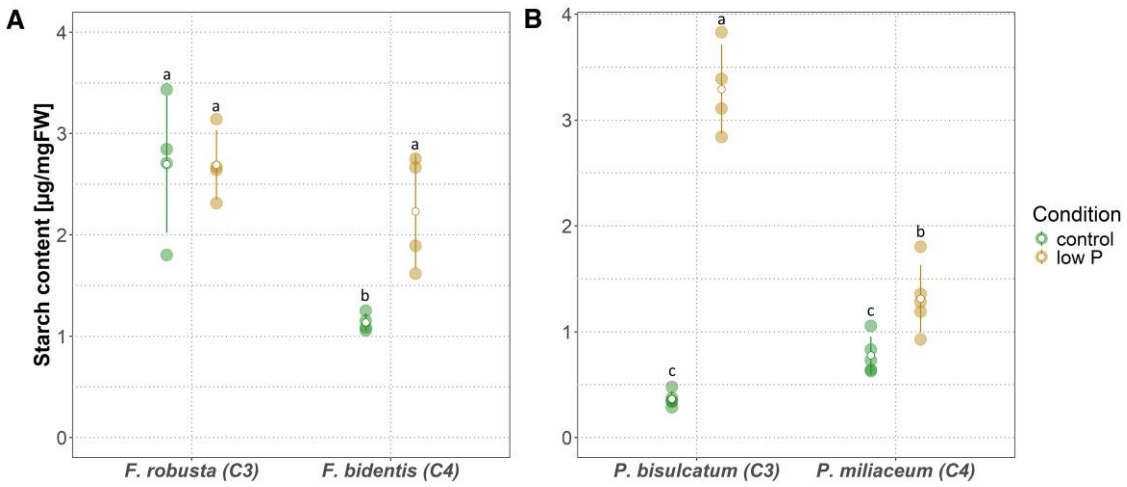

Figure 7. Accumulation of starch under phosphate starvation. Plants were grown for 4 wk (*Flaveria*) **A)** or 2 wk (*Panicum*) **B)** under low phosphate (2.5 µM) or control (200 µM) conditions, before the leaf material was harvested at the end of the light period and subjected to a colorimetric starch assay. Graphs show individual measurements as well as their mean and standard deviation ($n = 4$ to 5). Letters indicate significant differences ($P < 0.05$) based on a 2-way ANOVA followed by a Tukey's HSD test.

compared to the monocot *Panicum* C_3 and C_4 to see if it is an evolutionarily conserved trait. As a first observation under control conditions, the majority of phosphate was located in the roots in *Flaveria* and in the shoots in *Panicum* (Fig. 3, A and B). The accumulation of phosphate under deficiency conditions was similar between the species, indicating that C_3 and C_4 have similar sensitivity and uptake ability under starvation. Also, the phosphate uptake rates do not differ between C_3 and C_4 species under low phosphate conditions (Fig. 4). However, when comparing the distribution of phosphate between the below- and aboveground plant parts and especially when calculating the ratios from the PO_4 data, the trend seen for the *Flaveria* gradient above can be confirmed also for the monocot species. Both C_4 *F. bidentis* and *P. miliaceum* showed a higher accumulation in the leaves compared to their C_3 relatives, which suggests a general C_4 characteristic that is evolutionarily conserved at least between these 2 distinct genera and might be explained by several factors. The chloroplastic transporter exporting sugars in exchange with phosphate TPT is more abundant and has a higher flux in C_4 plants, which also possess the additional symporter requiring phosphate ions, the phosphoenolpyruvate/phosphate translocator (PPT) (Bräutigam et al. 2008). In C_4 plants, PPDK, which regenerates the CO_2 acceptor PEP, is a highly abundant protein with a much higher flux than in C_3 plants (Edwards et al. 1985). On the other hand, the higher demand for phosphate in leaves of C_4 might be due to its regulatory functions, since several enzymes involved in carbon assimilation in C_4 plants are regulated by phosphorylation (Jiao and Chollet 1991; Vidal and Chollet 1997). Furthermore, the generally higher growth rates in C_4 (Monteith 1978) might also lead to a higher demand for phosphate-containing structural compounds such as lipids, nucleotides, sugars, and proteins, which would increase the need for phosphate.

The total phosphorus levels under varying phosphate conditions reflect the results obtained for inorganic phosphate (Fig. 3, C and D). This shows that it is not only the phosphate uptake itself but the whole pool of phosphorus-containing metabolites including organically bound phosphorus that is adapted to the phosphate supply. When using these 2 data sets to calculate the pool size as percentage of the total phosphorus stored in phosphate, there was an overall slightly higher percentage in the shoots of both C_4 species *F. bidentis* and *P. miliaceum* in comparison to their C_3 relative (Supplementary Table S2). This would support the hypothesis that C_4 plants have a higher demand for the ion itself which is needed for the symporter activity and not for phosphorus-containing metabolites or structural compounds. Furthermore, both C_4 species showed a roughly constant percentage of P in PO_4 under differing phosphate conditions in their shoots (around 50%), while the percentage increased quite strongly with phosphate availability in their roots. Since PO_4 is the preferred storage form of phosphorus, one could speculate that under deficiency, C_4 plants do not store a lot of phosphorus taken up from the soil in their roots but rather directly transport it to the aboveground tissues where it is needed.

The differences in phosphate allocation due to the photosynthesis type were also supported by the expression analyses in roots of genes involved in phosphate uptake and distribution among the plant organs (Fig. 8). *PHO1*, a gene encoding a transporter involved in loading of phosphate to the xylem (Hamburger et al. 2002), showed higher expression in both C_4 species compared to their C_3 relatives, which correlated with their higher phosphate levels in the shoots indicating that PHO1 might be responsible for the elevated root-to-shoot translocation of phosphate in C_4 species. However, *PHO1* expression was not induced by the low phosphate treatment in any of the 4 species, possibly because it is regulated through a posttranslational mechanism. This matches previous studies on *Arabidopsis*, showing that PHO1 protein is degraded under phosphate limitation and PHO2 activity is crucial for this process (Liu et al. 2012). The *PHO2* gene codes for an E2 conjugase that is responsible for the negative regulation of several phosphate-responsive genes. Its transcript levels in *Arabidopsis* were shown to be reduced under phosphate limitation by microRNA399 as well as by an additional microRNA-independent mechanism (Bari et al. 2006). microRNA399, a shoot derived signal, is induced by phosphate limitation and responsible for induction of phosphate starvation responses (Fujii et al. 2005). Furthermore, microRNA399 was proposed to be transported from shoots to roots where it prevents accumulation of PHO2 that then induces a higher transport of phosphate from the roots to the shoots (Bari et al. 2006). The presented experiments could confirm this regulatory feedback loop, in particular for the monocot C_4 *P. miliaceum*, as it showed a strong induction of microRNA399 in roots under phosphate starvation (Fig. 8E) that led to a corresponding decrease in *PHO2* levels (Fig. 8B). PHTs have

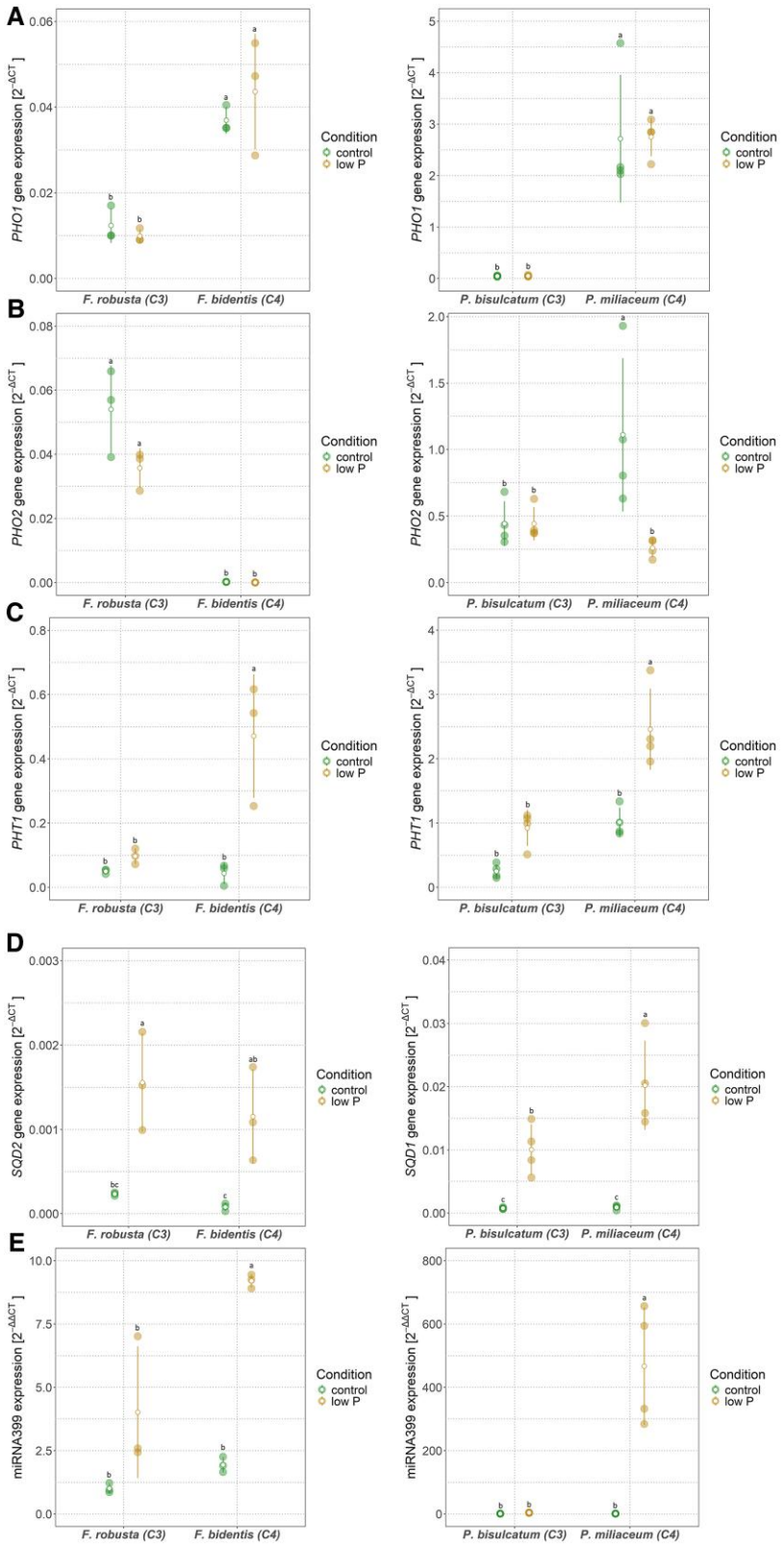

Figure 8. Regulation of key phosphate genes under phosphate starvation. Gene expression in roots of plants grown under low phosphate (2.5 μM) or control (200 μM) conditions was measured by RT-qPCR. Expression of PHO1 **A)**, PHO2 **B)**, PHT1 **C)**, and SQD **D)** were normalized to expression of housekeeping genes TIP41 or CYP5; miRNA399 **E)** transcript levels were normalized to expression of miRNA159 as well as the control. Graphs show individual measurements as well as their mean and standard deviation ($n = 3$ to 4). Letters indicate significant differences ($P < 0.05$) based on a 2-way ANOVA followed by a Tukey's HSD test.

been identified as high-affinity phosphate transporters in *Arabidopsis* roots that are involved in phosphate starvation response (Muchhal et al. 1996). However, PHT transporters are encoded by a big gene family with several candidates that differ in their location on the plant or cell level as well as their regulation (Nussaume et al. 2011). Incomplete genome annotation of the nonmodel plants

used in this study makes it hard to study these genes, since there are several homologous isoforms showing high sequence similarities and it is not yet clear which are the main responsible genes in *Flaveria* or *Panicum*. Nevertheless, gene expression analyses showed that *PHT1* is induced by phosphate limitation at least slightly in all 4 tested species, while there was a significant increase only in the 2 C_4 species. This could underline the higher demand of phosphate in C_4 discussed earlier.

Using interspecies grafts between C_3 and C_4 *Flaveria* species was instrumental in determining the role of root in control of sulfate allocation between shoots and roots (Gerlich et al. 2018). Therefore, we employed the grafts also for deeper analysis of the control of phosphate homeostasis. While the distribution of phosphate between the organs in C_3/C_4 heterografts was similar to the C_3/C_3 control, the C_4/C_3 heterograft showed a similar distribution as the C_4/C_4 homografts (Fig. 2). This indicates that the high accumulation of phosphate in C_4 leaves is controlled by the shoots. This is a surprising result since the internal and external phosphate status is initially sensed in the roots and signals are transported via the xylem to the shoots, where subsequent signals are induced and distributed through the plant via the phloem (Zhang et al. 2014).

The shoot-to-root ratio of phosphate was significantly increased by phosphate limitation in both *Flaveria* species and *P. miliaceum*, indicating that these plants induce a higher translocation of phosphate from the place of uptake to the leaves under these deficiency conditions and this was reversed in *P. bisulcatum* (Supplementary Fig. S4). In the model species *Arabidopsis thaliana*, inorganic phosphate accumulates to higher levels in shoots in comparison to roots under control conditions, while there is a balanced distribution between the organs under phosphate limitation (Bonnot et al. 2016). Hence, the reports on *Arabidopsis* are more comparable to the presented results for *P. bisulcatum*, suggesting that the observations are not specific for monocots and dicots but rather differ between individual species and genera.

Photosynthetic CO_2 fixation is inhibited by phosphate starvation only in the C_4 dicot

Given the higher demand for phosphate in C_4 species, evidenced by higher concentration in the leaves, it could be expected that the C_4 species would be more sensitive to phosphate limitation. We thus used gas exchange measurements to obtain specific CO_2 response curves as a measure of photosynthetic performance (Fig. 5, A and B). The initial slopes as well as the CO_2 compensation points were not affected by the phosphate level in any species, which shows that phosphate has no effect on the carboxylation efficiency of Rubisco or PEP carboxylase. The saturation phases of the curves and the maximal CO_2 assimilation rates (Fig. 5, C and D) revealed that only *F. bidentis* showed significantly impaired carbon fixation rates under phosphate starvation. This was unexpected because the different shoot/root ratio of phosphate between C_3 and C_4 species was observed in both *Flaveria* and *Panicum*.

What can be the reason for the specific sensitivity of *F. bidentis* to P limitation? Since the limitation in photosynthetic performance is not due to PEP carboxylase activity, the substrate availability might be limiting due to a decelerated ribulose-1,5-bisphosphate regeneration. CO_2 assimilation rates were shown to drop severely also in the C_4 crop plant maize exposed to phosphate limitation (Usuda and Shimogawara 1992). On the other hand, although low phosphate conditions were previously shown to reduce photosynthesis in a range of C_3 species including spinach, barley, and sugar beet (Dietz and Foyer 1986; Rao and Terry 1989), this seems not to be the case for the 2 C_3 plants in this study. However, different reports showed discrepant relations between phosphate limitation and performance of the C_3 and C_4 cycle. A similar study comparing grass species with different photosynthesis types revealed that CO_2 assimilation is less inhibited by phosphate limitation in C_4 than in C_3 while photosynthetic phosphate use efficiency increased under low phosphate stronger in C_4 (Ghannoum and Conroy 2007). Possibly, the C_4 grasses employ a more efficient intercellular allocation of phosphate between the vacuole and cytoplasm (Ghannoum and Conroy 2007). The Rubisco enzyme activity was shown to be reduced by phosphate deficiency in sunflower but not in maize (Jacob and Lawlor 1992), which matches our observations of the CO_2 assimilation data for monocots and dicots, since sunflower is very closely related to *Flaveria* while maize is closer to *Panicum*.

Thus, it seems that the C_4 photosynthetic cycle is more affected by limiting phosphate concentration, which matches the general view of lower phenotypic plasticity of C_4 plants, i.e. their lower efficiency in adapting to unfavorable conditions (Sage and McKown 2006). This seems to be true at least for the dicots and is probably due to their higher demand of phosphate for a successful C_4 cycle with all its transport processes. This is also in agreement with the higher phosphate allocation toward the leaves in C_4 plants which was discussed earlier. Furthermore, when comparing the 2 different C_4 systems, one can speculate that even though they both should have a higher phosphate demand for completing the C_4 cycle, the monocot C_4 seems to be better adapted by inducing microRNA399 under phosphate limitation to a higher level than the dicot and subsequently increasing phosphate starvation response to meet the higher phosphate demand. That could also explain why in comparison to the dicot C_4, the monocot C_4 is not affected in its carbon assimilation.

Downstream metabolic responses to phosphate limitation are not photosynthesis type specific but rather genus or species specific

Since phosphate is one of the essential nutrients for plants, its limitation affects multiple layers of plant metabolism. Indeed, a previously published metabolic profiling in *Arabidopsis* revealed 87 primary and 35 secondary metabolites being affected by phosphate limitation, including, for example, an increase of many amino acids, organic acids, and sugars (Pant et al. 2015). However, we hypothesized that different metabolic groups might be affected in C_3 and C_4 plants. For example, intermediates from the photorespiratory pathway such as serine, glycine, or glycolate might be more affected in C_3, while organic acids such as pyruvate, malate, and aspartate might show a stronger response in C_4. The presented GC-MS results showed that the accumulation of many amino acids, such as glutamate, phenylalanine, methionine, aspartate, glutamine, leucine, and serine, was strongly reduced by phosphate limitation in *F. robusta* but not in *F. bidentis*, which indicates that the amino acid metabolism is generally more affected by phosphate in the C_3 than it is in the C_4. The total amino acid content as the percentage of total C was shown to be almost 40% in *F. robusta* and only around 10% in *F. bidentis* (Borghi et al. 2022). This hints to a more important role of amino acids in the *Flaveria* C_3 that might also explain the elevated sensitivity of the amino acid pools to stress conditions.

Several organic acids and other TCA cycle intermediates including malate, fumarate, pyruvate, and malonate were significantly downregulated by phosphate limitation in *F. bidentis* but

not in *F. robusta* (Fig. 6). This indicated that due to the reduced assimilation of CO_2 in *F. bidentis*, also the flux of carbon into sugars is limited in these plants. On the other hand, citrate and isocitrate showed the opposite trend, since they were significantly upregulated by low phosphate but only in *F. robusta*. This might be because the CO_2 assimilation is not inhibited, so that the first intermediates of the TCA cycle can still be produced, but the light reaction might be impaired leading to reduced availability of ATP and NADPH, which is needed for the further conversion into sugars and that way early intermediates might accumulate.

Opposite to the trends in *Flaveria*, most measured metabolites showed elevated levels under phosphate depletion in comparison to the control in both *Panicum* species. Especially, most amino acids were very consistently upregulated in both *Panicum* species. This can be either due to a lower protein synthesis rate or to an induced degradation of proteins under low phosphate. Still some differences were observed within the *Panicum* genus. Malate and citramalate as well as the 2 sugars fructose and xylose were very highly upregulated by phosphate limitation in *P. bisulcatum* but not in *P. miliaceum*. This could lead to the conclusion that in the C_3 *Panicum*, the incorporation of assimilated carbon into organic compounds and subsequently into sugars might be impaired by an insufficient phosphate supply.

Starch functions as a storage form of assimilates but can also represent a sink for unused carbon. Indeed, previous studies showed that starch levels are increased under phosphate starvation because there is a decreased exchange of cytosolic phosphate with triose phosphate during low phosphate conditions, leading to accumulation of Calvin cycle intermediates and accelerated flux to starch (Li et al. 2021). This expectation could be confirmed for all tested species except for *F. robusta* (Fig. 7). However, the extent by which starch levels were elevated was very different. While in *P. bisulcatum*, the starch accumulation was 9 times higher under low phosphate, the level was only 1.7 times elevated in *P. miliaceum*. However, when comparing these 2 species under control conditions, there were no differences, while in *Flaveria*, the C_4 species showed a lower starch accumulation. Previous studies showed that in C_4 plants, starch synthesis and accumulation are located exclusively in the bundle sheath cells, while the accumulation differs strongly along the leaf blade (Majeran et al. 2010; Furbank and Kelly 2021). Hence, it is possible that the decreased starch levels in *F. bidentis* in comparison to its C_3 relative are due to the limitation of its synthesis in the bundle sheath. Furthermore, one could expect that the starch and sugar accumulation would be correlated, meaning that increased flux of carbon into starch would lead to a depletion of stored sugars. However, our data from the metabolite analyses did not support this hypothesis except *F. bidentis*, which showed increase in starch and a corresponding reduction in accumulation of sugars. The stronger response of starch accumulation in *F. bidentis* compared to *F. robusta* agrees well with the increased sensitivity to P limitation.

The metabolomics data make the distinction between the 2 dicots and monocots in response to P limitation very clear. In line with the CO_2 assimilation results, the *Flaveria* species seem to be more diverse while these traits were more conserved between species in *Panicum*, which might be due to differences in the evolutionary distance between the species within a genus. Furthermore, there seems to be a generally different coping strategy in monocots and dicots, since the monocots accumulated most of the metabolites including many sugars as well as TCA cycle intermediates during phosphate starvation, while in both dicot species, these metabolite levels were rather diminished. Interestingly, while there are no substantial differences in C_4 photosynthetic carbon metabolism between monocots and dicots, the nutritional pathways seem to be adapted to C_4 photosynthesis differently in these 2 groups as the bundle sheath-specific localization of enzymes for sulfate reduction described for many C_4 species (Gerwick et al. 1980) was shown to be specific to the monocots (Koprivova et al. 2001). In addition, in response to sulfur deficiency, the monocots are able to oxidize cysteine to sulfate, but the dicots do not (Rahimzadeh Karvansara et al. 2023).

Taken together, 2 main conclusions may be drawn here. Firstly, phosphate and phosphorus accumulation as well as expression of key phosphate genes indicated a higher demand of phosphate in shoots of C_4 plants. This seems to be a trait that was a necessary prerequisition or a consequence of the C_4 evolution and is presumably linked with the higher demand for phosphate to fuel the additional transport processes in the C_4 leaf. Secondly, the dicot C_4 was most affected by phosphate limitation on a physiological level indicated by a diminished photosynthesis rate while all 4 tested species were affected on a metabolic level (including primary metabolites, starch, and genes in lipid synthesis), but the metabolic responses were rather species or genus specific than specific for the photosynthesis type. The high level of induction of microRNA399 in the C_4 monocot seems to be responsible for its better adaptation to phosphate deficiency than the C_4 dicot.

Materials and methods

Plant material and cultivation

F. bidentis and *F. robusta* were grown in a liquid hydroponic system. Cuttings from adult plants were placed into 50 mL tubes covered in aluminum foil which contained the Hoagland media (Supplementary Table S3) with varying phosphate concentrations. Plants grew for 4 wk in a growth chamber under long-day (16 h light, 8 h dark) condition and a temperature of 31 °C during the day and 22 °C at night. The medium was changed first after 1 wk and then every 3 to 4 d.

P. bisulcatum and *P. miliaceum* seeds were surface sterilized with chlorine gas for 4 h and afterward placed onto ½ Murashige and Skoog (MS) (Duchefa, Haarlem, Netherlands) agar plates. After 7 to 10 d, seedlings were transferred into pots containing a 3:1 mix of vermiculite and autoclaved sand and watered with media described above. Plants grew for 2 wk in the same conditions as *Flaveria*.

Alternatively, seeds were sterilized with chlorine gas and placed onto agar plates containing ½ MS or Hoagland media. Seedlings grew in a growth camber under long-day (16 h light, 8 h dark) and a temperature of 31 °C during the day and 22 °C at night.

Interspecies micrografting of *F. robusta* and *F. bidentis*

Interspecies micrografting of *F. robusta* and *F. bidentis* was conducted as described in Gerlich et al. (2018), using the modified collar-free micrografting protocol by Marsch-Martínez et al. (2013) with seedlings 5 d after germination under sterile conditions. The seedlings were transferred onto small square petri dishes (120 mm × 120 mm × 15 mm) containing a thin layer (2 to 4 mm) of the liquid Hoagland medium. Cotyledons were removed with a single cut with a thin, commercial razor blade. Scion and stock were separated by a single horizontal cut in the upper third of the hypocotyl. Subsequently, the scion and stock were joined thoroughly as soon as possible on fresh small square petri dishes with the Hoagland medium, supplemented with 0.5% sucrose. Cutting and graft union was performed with the help of a Hund SM33 binocular stereoscope (Hund, Wetzlar). Fresh grafts were

incubated in a Percival phytochamber for 7 d with a slight tilt of the plates at 5° to 10° and subsequently moved to high-light conditions. Twelve days after grafting, the grafts were transferred to large, square petri dishes to grant suitable space for scion and stock development. Exposure to different nutrient conditions was conducted 29 d after grafting.

Metabolic analyses

For anion measurement, 25 to 30 mg root or leaf material was homogenized and extracted in 1 mL H_2O at 4 °C for 1 h. Afterward, samples were heated at 95 °C for 15 min and centrifuged for 20 min at 4 °C and maximum speed. The supernatant was diluted with water, and inorganic anions were separated on a Dionex IonPac AS22 RFIC 4× 250 mm analytic column and quantified with a Dionex ICS-1100 chromatography system (Thermo Fisher Scientific, Darmstadt, Germany). A 4.5 mM Na_2CO_3 and 1.4 mM $NaHCO_3$ were used as running buffers, and amounts were calculated based on an external standard curve as described by Dietzen et al. (2020).

Starch content was quantified in 30 mg leaf material, breaking down the starch enzymatically and quantifying the glucose colorimetrically using the Starch Assay Kit (Sigma-Aldrich) following the manufacturer's instructions.

Total soluble proteins were quantified by Bradford assay. A 20 mg plant material was extracted in 1 mL 0.1 M NaOH (pH 12.8) and centrifuged for 5 min. A 10 µL of the extract was mixed with 790 µL water as well as 200 µL Bradford dye (Bio-Rad, Hercules, United States) and incubated for 5 min. Absorbance at 595 nm was measured, and protein content was calculated based on a BSA protein standard curve.

For global metabolic analysis, around 40 mg shoot material was extracted in a mixture of H_2O:MeOH:$CHCl_3$ (1:2.5:1), vortexed, and shaken for 6 min at 4 °C. Samples were centrifuged for 5 min, and the supernatant was used for metabolite analysis by GC-MS using a 7200 GC-QTOF (Agilent, Santa Clara, United States) as described in Schlüter et al. (2023). For quantification, peak areas were normalized to Ribitol/DMPA as an internal standard.

Elemental analysis

Elemental analysis was conducted using 10 mg dried plant material, digesting it with 0.5 mL 67% nitric acid first at room temperature overnight and then at 95 °C until fully dissolved. Extracts were diluted with 4.5 mL H_2O and centrifuged for 1 h at 4000 rpm and 4 °C. The supernatant was subjected to an analysis using the Agilent 7700 Inductively Coupled Plasma Mass Spectrometer (Almario et al. 2017).

Phosphate uptake rate

For the uptake experiment, plants were germinated on ½ MS agar plates and transferred on Hoagland plates with specific phosphate concentrations for further 5 d. Afterward, they were placed into 2 mL tubes containing the media with adjusted phosphate concentration for another 2 d. The medium was exchanged for media supplemented with 100 µCi ^{33}P, and the plants were incubated for 30 min, before all plant parts were harvested and extracted in 1 mL 0.1 M HCl. After centrifugation, 200 µL of the extracts was used to determine the ^{33}P phosphate content with use of a scintillation counter.

Photosynthetic efficiency by an infrared gas analyzer

Photosynthetic parameters were measured in fully expanded leaves of hydroponically grown plants with an infrared gas analyzer within the Portable Photosynthesis System LICOR 6400XT (LI-COR Biosciences, Lincoln, United States). Conditions were set to 25 °C, VPD of 1.5 kPa, fan speed of 10,000 rpm, flow rate of 400 µmol/s, and light at 1500 µmol/m^2s. The CO_2 response was measured in a range from 10 to 1500 µmol/mol.

Gene expression

Total RNA of the root material was extracted using phenol-chloroform-isoamyl alcohol extraction and LiCl precipitation. cDNA was synthesized with the RevertAid RT Reverse Transcription Kit (Thermo Fisher Scientific, Darmstadt, Germany) following the manufacturer's instructions. Gene expression was determined using SYBR Green and the CFX96 Touch Real-Time PCR Detection System (Bio-Rad, Hercules, United States). Primers were obtained from Sigma-Aldrich and can be found in Supplementary Table S4. For expression analysis of microRNA, a RT reaction with specific primer was performed and an adapted RT-qPCR protocol was utilized exactly as described in Varkonyi-Gasic et al. (2007).

Accession numbers

Sequence data from this article can be found in the GenBank/EMBL data libraries under accession numbers GCA_018326485.1 for *F. robusta*, GCA_018326385.1 for *F. bidentis*, and GCA_038442765.1 for *P. miliaceum*.

Acknowledgments

We thank S. Ambrosius for the technical support. We also thank the Biocenter MS Platform Cologne for the measurements of mineral composition and the CEPLAS Metabolism and Metabolomics Laboratory for the analysis of primary metabolites. R.K. gratefully acknowledges the support from the International Max Planck Research School on "Understanding Complex Plant Traits Using Computational and Evolutionary Approaches."

Author contributions

S.K., R.K., and S.G. conceived and designed the research. R.K., S.G., M.M., A.K., and P.W. performed the experiments. R.K. drafted the manuscript and prepared figures. All authors were involved in revising the manuscript.

Supplementary data

The following materials are available in the online version of this article.

Supplementary Figure S1. Phosphate and total phosphorus levels in *Flaveria* species along the evolutionary gradient from C_3 to C_4.

Supplementary Figure S2. Phosphate uptake rates in *Flaveria* grafts.

Supplementary Figure S3. Fresh weight under gradient of phosphate conditions.

Supplementary Figure S4. Ratio of phosphate between shoots and roots.

Supplementary Figure S5. Nitrate content under various phosphate conditions.

Supplementary Figure S6. Sulfate content under various phosphate conditions.

Supplementary Figure S7. Ionomics.

Supplementary Figure S8. Iron content under various phosphate conditions.

Supplementary Figure S9. Manganese content under various phosphate conditions.

Supplementary Table S1. Metabolite concentrations.

Supplementary Table S2. Percentage of phosphate in total phosphorus.

Supplementary Table S3. Composition of the Hoagland media.

Supplementary Table S4. Primer sequences.

Funding

This work was supported by the Deutsche Forschungsgemeinschaft (DFG) under Germany's Excellence Strategy—EXC 2048/1—project 390686111 (S.K., S.G., A.K., P.W.) and a project 436380415 (S.K., R.K., M.M.).

Conflict of interest statement. None declared.

Data availability

The data underlying this article are available in the article and in its online supplementary material.

References

Almario J, Jeena G, Wunder J, Langen G, Zuccaro A, Coupland G, Bucher M. Root-associated fungal microbiota of nonmycorrhizal *Arabis alpina* and its contribution to plant phosphorus nutrition. *Proc Natl Acad Sci U S A*. 2017:114(44):E9403–E9412. https://doi.org/10.1073/pnas.1710455114

Atkinson RRL, Mockford EJ, Bennett C, Christin P-A, Spriggs EL, Freckleton RP, Thompson K, Rees M, Osborne CP. C4 photosynthesis boosts growth by altering physiology, allocation and size. *Nat Plants*. 2016:2(5):16038. https://doi.org/10.1038/nplants.2016.38

Bari R, Datt Pant B, Stitt M, Scheible W-R. PHO2, microRNA399, and PHR1 define a phosphate-signaling pathway in plants. *Plant Physiol*. 2006:141(3):988–999. https://doi.org/10.1104/pp.106.079707

Bonnot C, Pinson B, Clément M, Bernillon S, Chiarenza S, Kanno S, Kobayashi N, Delannoy E, Nakanishi TM, Nussaume L, *et al*. A chemical genetic strategy identify the PHOSTIN, a synthetic molecule that triggers phosphate starvation responses in *Arabidopsis thaliana*. *New Phytol*. 2016:209(1):161–176. https://doi.org/10.1111/nph.13591

Borghi GL, Arrivault S, Günther M, Barbosa Medeiros D, Dell'Aversana E, Fusco GM, Carillo P, Ludwig M, Fernie AR, Lunn JE, *et al*. Metabolic profiles in C3, C3-C4 intermediate, C4-like, and C4 species in the genus *Flaveria*. *J Exp Bot*. 2022:73(5):1581–1601. https://doi.org/10.1093/jxb/erab540

Bräutigam A, Hoffmann-Benning S, Weber APM. Comparative proteomics of chloroplast envelopes from C3 and C4 plants reveals specific adaptations of the plastid envelope to C4 photosynthesis and candidate proteins required for maintaining C4 metabolite fluxes. *Plant Physiol*. 2008:148(1):568–579. https://doi.org/10.1104/pp.108.121012

Dietz K-J, Foyer C. The relationship between phosphate status and photosynthesis in leaves. *Planta*. 1986:167(3):376–381. https://doi.org/10.1007/BF00391342

Dietzen C, Koprivova A, Whitcomb SJ, Langen G, Jobe TO, Hoefgen R, Kopriva S. The transcription factor EIL1 participates in the regulation of sulfur-deficiency response. *Plant Physiol*. 2020:184(4):2120–2136. https://doi.org/10.1104/pp.20.01192

Edwards GE, Gutierrez M. Metabolic activities in extracts of mesophyll and bundle sheath cells of *Panicum miliaceum* (L.) in relation to the C(4) dicarboxylic acid pathway of photosynthesis. *Plant Physiol*. 1972:50(6):728–732. https://doi.org/10.1104/pp.50.6.728

Edwards GE, Nakamoto H, Burnell JN, Hatch MD. Pyruvate Pi dikinase and NADP-malate dehydrogenase in C4 photosynthesis: properties and mechanism of light/dark regulation. *Annual Reviews in Plant Physiology*. 1985:36:255–286. https://doi.org/10.1146/annurev.pp.36.060185.001351

Ermakova M, Danila FR, Furbank RT, von Caemmerer S. On the road to C4 rice: advances and perspectives. *Plant J*. 2020:101(4):940–950. https://doi.org/10.1111/tpj.14562

Essigmann B, Güler S, Narang RA, Linke D, Benning C. Phosphate availability affects the thylakoid lipid composition and the expression of SQD1, a gene required for sulfolipid biosynthesis in *Arabidopsis thaliana*. *Proc Natl Acad Sci U S A*. 1998:95(4):1950–1955. https://doi.org/10.1073/pnas.95.4.1950

Fliege R, Flügge UI, Werdan K, Heldt HW. Specific transport of inorganic phosphate, 3-phosphoglycerate and triosephosphates across the inner membrane of the envelope in spinach chloroplasts. *Biochim Biophys Acta*. 1978:502(2):232–247. https://doi.org/10.1016/0005-2728(78)90045-2

Fujii H, Chiou T-J, Lin S-I, Aung K, Zhu J-K. A miRNA involved in phosphate-starvation response in *Arabidopsis*. *Curr Biol*. 2005:15(22):2038–2043. https://doi.org/10.1016/j.cub.2005.10.016

Furbank RT, Kelly S. Finding the C4 sweet spot: cellular compartmentation of carbohydrate metabolism in C4 photosynthesis. *J Exp Bot*. 2021:72(17):6018–6026. https://doi.org/10.1093/jxb/erab290

Gerlich SC, Walker BJ, Krueger S, Kopriva S. Sulfate metabolism in C_4 *Flaveria* species is controlled by the root and connected to serine biosynthesis. *Plant Physiol*. 2018:178(2):565–582. https://doi.org/10.1104/pp.18.00520

Gerwick BC, Ku SB, Black CC. Initiation of sulfate activation: a variation in C_4 photosynthesis plants. *Science*. 1980:209(4455):513–515. https://doi.org/10.1126/science.209.4455.513

Ghannoum O, Conroy JP. Phosphorus deficiency inhibits growth in parallel with photosynthesis in a C3 (*Panicum laxum*) but not two C4 (*P. coloratum* and *Cenchrus ciliaris*) grasses. *Funct Plant Biol*. 2007:34(1):72. https://doi.org/10.1071/FP06253

Hamburger D, Rezzonico E, MacDonald-Comber Petétot J, Somerville C, Poirier Y. Identification and characterization of the *Arabidopsis* PHO1 gene involved in phosphate loading to the xylem. *Plant Cell*. 2002:14(4):889–902. https://doi.org/10.1105/tpc.000745

Hatch MD. C4 photosynthesis: a unique blend of modified biochemistry, anatomy and ultrastructure. *Biochim Biophys Acta (BBA)—Rev Bioenerget*. 1987:895(2):81–106. https://doi.org/10.1016/S0304-4173(87)80009-5

Heldt HW, Flügge U-I, Borchert S. Diversity of specificity and function of phosphate translocators in various plastids. *Plant Physiol*. 1991:95(2):341–343. https://doi.org/10.1104/pp.95.2.341

Jacob J, Lawlor DW. Dependence of photosynthesis of sunflower and maize leaves on phosphate supply, ribulose-1,5-bisphosphate carboxylase/oxygenase activity, and ribulose-1,5-bisphosphate pool size. *Plant Physiol*. 1992:98(3):801–807. https://doi.org/10.1104/pp.98.3.801

Jiao J, Chollet R. Posttranslational regulation of phosphoenolpyruvate carboxylase in C_4 and crassulacean acid metabolism plants. *Plant Physiol*. 1991:95(4):981–985. https://doi.org/10.1104/pp.95.4.981

Jobe TO, Rahimzadeh Karvansara P, Zenzen I, Kopriva S. Ensuring nutritious food under elevated CO_2 conditions: a case for improved C4 crops. *Front Plant Sci*. 2020:11:1267. https://doi.org/10.3389/fpls.2020.01267

Jobe TO, Zenzen I, Rahimzadeh Karvansara P, Kopriva S. Integration of sulfate assimilation with carbon and nitrogen metabolism in transition from C3 to C4 photosynthesis. *J Exp Bot*. 2019:70(16):4211–4221. https://doi.org/10.1093/jxb/erz250

Kennedy RA, Laetsch WM. Plant species intermediate for C3, C4 photosynthesis. *Science*. 1974:184(4141):1087–1089. https://doi.org/10.1126/science.184.4141.1087

Koprivova A, Melzer M, von Ballmoos P, Mandel T, Brunold C, Kopriva S. Assimilatory sulfate reduction in C3, C3-C4, and C4 species of *Flaveria*. *Plant Physiol*. 2001:127(2):543–550. https://doi.org/10.1104/pp.010144

Ku MSB, Wu J, Dai Z, Scott RA, Chu C, Edwards GE. Photosynthetic and photorespiratory characteristics of *Flaveria* species. *Plant Physiol*. 1991:96(2):518–528. https://doi.org/10.1104/pp.96.2.518

Li J, Du A, Liu P, Tian X, Jin Y, Yi Z, He K, Fang Y, Zhao H. High starch accumulation mechanism and phosphorus utilization efficiency of duckweed (*Landoltia punctata*) under phosphate starvation. *Ind Crops Prod*. 2021:167:113529. https://doi.org/10.1016/j.indcrop.2021.113529

Liu T-Y, Huang T-K, Tseng C-Y, Lai Y-S, Lin S-I, Lin W-Y, Chen J-W, Chiou T-J. PHO2-Dependent degradation of PHO1 modulates phosphate homeostasis in *Arabidopsis*. *Plant Cell*. 2012:24(5):2168–2183. https://doi.org/10.1105/tpc.112.096636

Loladze I. Hidden shift of the ionome of plants exposed to elevated CO_2 depletes minerals at the base of human nutrition. *eLife*. 2014:3:e02245. https://doi.org/10.7554/eLife.02245

Lundgren MR, Osborne CP, Christin P-A. Deconstructing Kranz anatomy to understand C4 evolution. *J Exp Bot*. 2014:65(13):3357–3369. https://doi.org/10.1093/jxb/eru186

Maathuis FJ. Physiological functions of mineral macronutrients. *Curr Opin Plant Biol*. 2009:12(3):250–258. https://doi.org/10.1016/j.pbi.2009.04.003

Majeran W, Friso G, Ponnala L, Connolly B, Huang M, Reidel E, Zhang C, Asakura Y, Bhuiyan NH, Sun Q, *et al*. Structural and metabolic transitions of C4 leaf development and differentiation defined by microscopy and quantitative proteomics in maize. *Plant Cell*. 2010:22(11):3509–3542. https://doi.org/10.1105/tpc.110.079764

Marsch-Martínez N, Franken J, Gonzalez-Aguilera KL, de Folter S, Angenent G, Alvarez-Buylla ER. An efficient flat-surface collar-free grafting method for *Arabidopsis thaliana* seedlings. *Plant Methods*. 2013:9(1):14. https://doi.org/10.1186/1746-4811-9-14

Monteith JL. Reassessment of maximum growth rates for C3 and C4 crops. *Exp Agric*. 1978:14(1):1–5. https://doi.org/10.1017/S0014479700008255

Moore R, Black CC. Nitrogen assimilation pathways in leaf mesophyll and bundle sheath cells of C4 photosynthesis plants formulated from comparative studies with *Digitaria sanguinalis* (L.) Scop. 1. *Plant Physiol*. 1979:64(2):309–313. https://doi.org/10.1104/pp.64.2.309

Muchhal US, Pardo JM, Raghothama KG. Phosphate transporters from the higher plant *Arabidopsis thaliana*. *Proc Natl Acad Sci U S A*. 1996:93(19):10519–10523. https://doi.org/10.1073/pnas.93.19.10519

Mueller ND, Gerber JS, Johnston M, Ray DK, Ramankutty N, Foley JA. Closing yield gaps through nutrient and water management. *Nature*. 2012:490(7419):254–257. https://doi.org/10.1038/nature11420

Nussaume L, Kanno S, Javot H, Marin E, Pochon N, Ayadi A, Nakanishi TM, Thibaud M-C. Phosphate import in plants: focus on the PHT1 transporters. *Front Plant Sci*. 2011:2:83. https://doi.org/10.3389/fpls.2011.00083

Oliver N, Avramov AP, Nürnberg DJ, Dau H, Burnap RL. From manganese oxidation to water oxidation: assembly and evolution of the water-splitting complex in photosystem II. *Photosynth Res*. 2022:152(2):107–133. https://doi.org/10.1007/s11120-022-00912-z

Pant B-D, Pant P, Erban A, Huhman D, Kopka J, Scheible W-R. Identification of primary and secondary metabolites with phosphorus status-dependent abundance in *Arabidopsis*, and of the transcription factor PHR1 as a major regulator of metabolic changes during phosphorus limitation. *Plant Cell Environ*. 2015:38(1):172–187. https://doi.org/10.1111/pce.12378

Powell AM. Systematics of *Flaveria* (Flaveriinae—Asteraceae). *Ann Mo Bot Gard*. 1978:65(2):590–636. https://doi.org/10.2307/2398862

Rahimzadeh Karvansara P, Kelly C, Krone R, Zenzen I, Ristova D, Silz E, Jobe TO, Kopriva S. Unique features of regulation of sulfate assimilation in monocots. *J Exp Bot*. 2023:74(1):308–320. https://doi.org/10.1093/jxb/erac402

Rao IM, Terry N. Leaf phosphate status, photosynthesis, and carbon partitioning in sugar beet: I. Changes in growth, gas exchange, and Calvin cycle enzymes. *Plant Physiol*. 1989:90(3):814–819. https://doi.org/10.1104/pp.90.3.814

Rezaei EE, Webber H, Asseng S, Boote K, Durand JL, Ewert F, Martre P, MacCarthy DS. Climate change impacts on crop yields. *Nat Rev Earth Environ*. 2023:4(12):831–846. https://doi.org/10.1038/s43017-023-00491-0

Sage RF. The evolution of C_4 photosynthesis. *New Phytol*. 2004:161(2):341–370. https://doi.org/10.1111/j.1469-8137.2004.00974.x

Sage RF, McKown AD. Is C4 photosynthesis less phenotypically plastic than C3 photosynthesis?. *J Exp Bot*. 2006:57(2):303–317. https://doi.org/10.1093/jxb/erj040

Sage RF, Pearcy RW, Seemann JR. The nitrogen use efficiency of C3 and C4 plants: III. Leaf Nitrogen effects on the activity of carboxylating enzymes in *Chenopodium album* (L.) and *Amaranthus retroflexus* (L.). *Plant Physiol*. 1987:85(2):355–359. https://doi.org/10.1104/pp.85.2.355

Schlüter U, Bouvier JW, Guerreiro R, Malisic M, Kontny C, Westhoff P, Stich B, Weber APM. Brassicaceae display variation in efficiency of photorespiratory carbon-recapturing mechanisms. *J Exp Bot*. 2023:74(21):6631–6649. https://doi.org/10.1093/jxb/erad250

Slack CR, Hatch MD, Goodchild DJ. Distribution of enzymes in mesophyll and parenchyma-sheath chloroplasts of maize leaves in relation to the C4-dicarboxylic acid pathway of photosynthesis. *Biochem J*. 1969:114(3):489–498. https://doi.org/10.1042/bj1140489

Sternberg LDSL, Deniro MJ, Sloan ME, Black CC. Compensation point and isotopic characteristics of C_3/C_4 intermediates and hybrids in *Panicum*. *Plant Physiol*. 1986:80(1):242–245. https://doi.org/10.1104/pp.80.1.242

Usuda H, Shimogawara K. Phosphate deficiency in maize: III. Changes in enzyme activities during the course of phosphate deprivation. *Plant Physiol*. 1992:99(4):1680–1685. https://doi.org/10.1104/pp.99.4.1680

van Dijk M, Morley T, Rau ML, Saghai Y. A meta-analysis of projected global food demand and population at risk of hunger for the period 2010–2050. *Nat Food*. 2021:2(7):494–501. https://doi.org/10.1038/s43016-021-00322-9

Varkonyi-Gasic E, Wu R, Wood M, Walton EF, Hellens RP. Protocol: a highly sensitive RT-PCR method for detection and quantification of microRNAs. *Plant Methods*. 2007:3:12. https://doi.org/10.1186/1746-4811-3-12

Vidal J, Chollet R. Regulatory phosphorylation of C4 PEP carboxylase. *Trends Plant Sci*. 1997:2(6):230–237. https://doi.org/10.1016/S1360-1385(97)89548-9

Yang X, Liu C, Liang C, Wang T, Tian J. The phosphorus-iron nexus: decoding the nutrients interaction in soil and plant. *Int J Mol Sci*. 2024:25(13):6992. https://doi.org/10.3390/ijms25136992

Zhang Z, Liao H, Lucas WJ. Molecular mechanisms underlying phosphate sensing, signaling, and adaptation in plants: phosphate sensing and signaling in plants. *J Integr Plant Biol*. 2014:56(3):192–220. https://doi.org/10.1111/jipb.12163

Zhu C, Kobayashi K, Loladze I, Zhu J, Jiang Q, Xu X, Liu G, Seneweera S, Ebi KL, Drewnowski A, *et al*. Carbon dioxide (CO_2) levels this century will alter the protein, micronutrients, and vitamin content of rice grains with potential health consequences for the poorest rice-dependent countries. *Sci Adv*. 2018:4(5):eaaq1012. https://doi.org/10.1126/sciadv.aaq1012